A&A 488, L21–L24 (2008)
DOI: 10.1051/0004-6361:200810303

Astronomy & Astrophysics

Letter to the Editor

First detection of CO lines in a water fountain star

J. H. He[1,2], H. Imai[3], T. I. Hasegawa[1], S. W. Campbell[1,4], and J. Nakashima[5]

[1] Institute of Astronomy and Astrophysics, Academia Sinica, PO Box 23-141, Taipei 10617, Taiwan
e-mail: jhhe@asiaa.sinica.edu.tw
[2] National Astronomical Observatories/Yunnan Observatory, Chinese Academy of Sciences, PO Box 110, Kunming, Yunnan Province 650011, PR China
[3] Department of Physics, Faculty of Science, Kagoshima University, 1-21-35 Korimoto, Kagoshima 890-0065, Japan
[4] Centre for Stellar and Planetary Astrophysics, School of Mathematical Sciences, Monash University, 3800 Melbourne, Australia
[5] Department of Physics, University of Hong Kong, Pokfulam Road, Hong Kong

Received 2 June 2008 / Accepted 14 July 2008

ABSTRACT

Context. Water fountain stars are very young post-AGB stars with high velocity water maser jets. They are the best objects in which to study the onset of bipolar jets from evolved stars due to their young dynamical ages. However, none of them has been observed in any thermal lines.
Aims. We aim to search for CO lines in the water fountain star IRAS 16342-3814 and investigate the properties of its thermal gas.
Methods. The proximity, peculiar stellar velocity and high Galactic latitude of IRAS 16342-3814 make a single dish observation possible. We use the Arizona Radio Observatory 10 m telescope to observe the CO $J = 2-1$ line and compare the line parameters with those of masers.
Results. We report the detection of ^{12}CO and ^{13}CO $J = 2-1$ lines from IRAS 16342-3814. The inferred ^{12}CO mass loss rate is an order of magnitude lower than the infrared and OH mass loss rates, indicating a very cold and thick O-rich circumstellar envelope around the star. We also find a ^{12}CO expansion velocity of $V_{\rm exp} = 46 \pm 1\,{\rm km\,s^{-1}}$ that is too high for an AGB wind and confirm the systemic velocity of $44 \pm 1\,{\rm km\,s^{-1}}$. In addition we measure a very low ^{12}CO/^{13}CO line ratio of 1.7.
Conclusions. The first detection of CO lines has provided a new way to investigate water fountain stars. Given the high expansion velocity of the CO gas and its relation to maser velocities, we infer that the CO emission region is co-located with the OH mainline masers in the warm base of the optical bipolar lobes, while the high velocity OH 1612 MHz and H_2O masers are located in the side walls and at the farthest ends of the bipolar lobes, respectively. Further observations are highly desirable to understand the very low ^{12}CO/^{13}CO line ratio.

Key words. stars: AGB and post-AGB – stars: circumstellar matter – stars: evolution – stars: individual: IRAS 16342-3814 – stars: winds, outflows – radio lines: stars

1. Introduction

Water fountain stars are a group of rare objects that display a thick circumstellar envelope (CSE) that is typical of asymptotic giant branch (AGB) stars and also high velocity bipolar jets ($\gtrsim$100 km s^{-1}) detected via their H_2O masers. They could be stars near the end of the AGB or post-AGB evolution stage when non-spherical circumstellar structures begin to develop inside the relic of the spherical AGB circumstellar envelope. Currently only about 10 such objects have been discovered through single dish and interferometry observations of their OH, H_2O and SiO masers (see the review by Imai 2007). However, none of them have ever been detected in a thermal molecular line. In this letter, we report the first detection of the $J = 2-1$ transition of ^{12}CO and ^{13}CO in the water fountain star IRAS 16342-3814.

IRAS 16342-3814 was discovered by Likkel & Morris (1988) to show H_2O masers with a line-of-sight expansion velocity up to 117.4 km s^{-1}, much higher than the typical speed of ~15 km s^{-1} for a spherical AGB wind (see, e.g., Chen et al. 2001). They also found a progressive increase of expansion velocity in OH masers, from 36 km s^{-1} (1665 MHz) through 42 km s^{-1} (1667 MHz) to 58 km s^{-1} (1612 MHz). The symmetrical H_2O maser velocities found by Likkel et al. (1992) allowed them to determine a star velocity of $V_{\rm sys} = 43.2 \pm 0.9\,{\rm km\,s^{-1}}$, which further constrained a higher line-of-sight H_2O maser expansion velocity of 130 km s^{-1}.

Optical and infrared imaging of this star has revealed striking structures in its CSE. The Hubble Space Telescope (HST) observations by Sahai et al. (1999) revealed a bipolar nebula. Corkscrew patterns were found in the bipolar lobes in follow-up infrared $L_{\rm p}$ band imaging with the Keck telescope (Sahai et al. 2005), indicating that the bipolar lobes and the H_2O masers might be created by precessing jets. Infrared imaging in the 3.8~20 μ range by Dijkstra et al. (2003) showed the variation of the CSE morphologies from bipolar at near infrared to spherical at middle infrared, demonstrating that the outer CSE ejected earlier was spherical and the star is currently undergoing CSE morphology transformation. Dijkstra et al. (2003) also found from the 2~200 μ Infrared Space Observatory (ISO) spectra that the star is the only object known to show absorption in both amorphous and crystalline silicate features. The very red spectral energy distribution possibly indicates a very cold and thick dusty CSE with an AGB mass loss rate of the order of $10^{-3}\,M_\odot\,{\rm yr^{-1}}$ (Dijkstra et al. 2003).

Interferometric measurements of masers have supplied kinematic information. The mapping of OH masers in IRAS 16342-3814 by Sahai et al. (1999) and Zijlstra et al. (2001) showed a

linear increase of line-of-sight outflow velocity with projected distance from the central star. High-velocity OH maser spots are located around the optical bipolar lobes while low-velocity maser spots appear near a dark waist close to the central star. These facts are in accord with a wind interaction model of the bipolar structure (Zijlstra et al. 2001). However, the corkscrew pattern in the infrared images also suggests that precessing jets may play some role. Very Long Baseline Array (VLBA) mapping of H_2O masers by Morris et al. (2003) and Claussen et al. (2004) showed a bipolar distribution of maser spot clusters with more than 2″ separation along the optical bipolar lobes and quasi-linear alignment of maser spots that delineates the shock front of the jets. The interplay between the jets and magnetic field is still unclear, although an extremely high degree of polarisation has been found in the OH masers (Te Lintel Hekkert et al. 1988; Szymczak & Gérard 2004).

The post-AGB nature of IRAS 16342-3814 has been critically investigated by Sahai et al. (1999). However the status of thermal gas in the CSE of this star is still unclear due to the lack of thermal molecular line observations. Unlike other known water fountain stars, IRAS 16342-3814 is the easiest object in which to search for CO lines with a single dish telescope, because it is relatively near, with a distance of 0.7 ∼ 2 kpc (Sahai et al. 1999; Zijlstra et al. 2001), it has a high galactic latitude of 5.°8 and a large line-of-sight velocity difference of at least 40 km s^{-1} from that of nearby interstellar molecular clouds.

2. Observation and data reduction

The ALMA band-6 sideband separating receiver on the Arizona Radio Observatory 10 m submillimeter telescope (SMT) was used for the ^{12}CO and ^{13}CO $J = 2-1$ observations towards IRAS 16342-3814 on 2008, May 09. Sky subtraction was made in beam switch mode with a 2 arcmin throw at 2.2 Hz in the azimuth direction. The receiver temperature was about 100−120 K. Two filter banks (FFBs, 1 GHz width, 1024 channels) were used for the two polarisations of the ^{12}CO line and two acousto-optical spectrometers (AOSs, 972.8 MHz width, 2048 channels) were used for the two polarisations of the ^{13}CO line. A 90 min integration under a $\tau_{225} = 0.15$ and a $T_{\rm sys} = 445$ K at a low elevation of 19° resulted in an rms noise of about 10 mK at a resolution of 3 MHz in each polarisation. Main beam efficiencies of 0.7 and 0.6 were used to convert the measured $T_{\rm A}^*$ into main beam temperature $T_{\rm mb}$ for the USB (^{12}CO) and LSB (^{13}CO), respectively. A telescope efficiency of 31 Jy/K was used to derive line peak flux. The beam width is about 32″ at both lines.

The GILDAS/CLASS package was used to reduce and analyse the data. The two polarisations were combined to improve the S/N. A zero order baseline was removed from each spectrum. We also experimented with a higher order baseline, but not much difference was found at the band center where the CO lines appear. The SHELL method in the CLASS package was used to fit both lines with a truncated parabolic line profile.

3. Results

The resulting spectra of ^{12}CO and ^{13}CO $J = 2-1$ lines are shown in Fig. 1, where each spectrum has been box smoothed to a resolution of ∼3 MHz. We do not see any strong interstellar emission or absorption signatures. Line profile fitting of ^{12}CO line gives a peak temperature of $T_{\rm mb} = 29$ mK (with rms = 7 mK), corresponding to a peak flux of 0.90 Jy (with rms = 0.22 Jy). The line area is 2.14 ± 0.14 K km s^{-1}, representing a 15σ detection

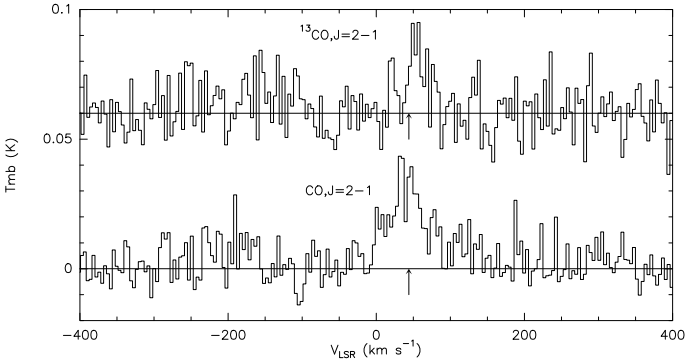

Fig. 1. The observed ^{12}CO and ^{13}CO 2−1 line profiles. The spectra have been box smoothed to a resolution of about 3 MHz. The ^{13}CO 2−1 line has been shifted upward by 0.06 K for clarity. The arrows mark $V_{\rm sys} = 44$ km s^{-1} that is derived from the ^{12}CO line.

of the line. A systemic velocity of $V_{\rm sys}(^{12}{\rm CO}) = 44 \pm 1$ km s^{-1} and a high expansion velocity of $V_{\rm exp}(^{12}{\rm CO}) = 46 \pm 1$ km s^{-1} are measured by line profile fitting. The $V_{\rm sys}(^{12}{\rm CO})$ agrees well with the H_2O maser systemic velocity of 43.2 ± 0.9 km s^{-1} from Likkel et al. (1992). We also notice a pair of narrow features near the centre of the ^{12}CO 2−1 line profile. However, because of the poor S/N, we are not sure if they are real features.

The ^{13}CO 2−1 spectrum is more noisy. We find from line profile fitting a line peak temperature of $T_{\rm mb}(^{13}{\rm CO}) = 17$ mK (with rms = 9 mK), corresponding to a peak flux of 0.53 Jy (with rms = 0.28 Jy). The line area of 1.02 ± 0.17 K km s^{-1} represents a 6σ detection of the line. The stellar velocity and CSE expansion velocity found from line profile fitting are $V_{\rm sys}(^{13}{\rm CO}) = 50 \pm 3$ km s^{-1} and $V_{\rm exp}(^{13}{\rm CO}) = 34 \pm 2$ km s^{-1}. The velocity differences between the ^{12}CO and ^{13}CO 2−1 lines could be merely caused by underestimated noise in the spectra.

4. Discussion

4.1. The low ^{12}CO mass loss rate

The detection of the ^{12}CO 2−1 line allows us to directly estimate the mass loss rate of IRAS 16342-3814. Using the ^{12}CO 2−1 formula scaled by Heske et al. (1990) from a ^{12}CO 1–0 formula postulated by Knapp & Morris (1985), we derive $\dot{M}(^{12}{\rm CO}) = 0.7 \sim 5.6 \times 10^{-6}\ M_\odot\ {\rm yr}^{-1}$ for a source distance of 0.7 ∼ 2 kpc. As discussed in Sect. 4.2, the detected CO gas may not represent the spherical AGB wind. The true AGB wind CO mass loss rate, if also estimated with Heske's formula, should be even lower than this value, because the CO gas emission from the slow AGB wind has not been definitely detected yet, while the mass loss rate is $\propto V_{\rm exp}^2 T_{\rm mb}({\rm CO})$. However, the formula of Baud & Habing (1983) applied to an OH 1612 MHz maser peak flux of 9 Jy (Likkel & Morris 1988) yields a much higher mass loss rate of $\dot{M}({\rm OH}) = 1.7{\sim}4.9 \times 10^{-5}\ M_\odot\ {\rm yr}^{-1}$ (with $V_{\rm exp} = 46$ km s^{-1} from our ^{12}CO line). Do et al. (2007) fitted the Spitzer MIPS 70 μ images with a two shell model, and obtained $\dot{M}(70\ \mu) = 0.4{\sim}3 \times 10^{-5}\ M_\odot\ {\rm yr}^{-1}$ for an inner smooth CSE and $\dot{M}({\rm shell}) = 0.4{\sim}3 \times 10^{-4}\ M_\odot\ {\rm yr}^{-1}$ for an outer extended dust shell (assuming a gas-to-dust mass ratio of 200 and $V_{\rm exp} = 15$ km s^{-1}. Here we note that our measured ^{12}CO expansion velocity of 46 km s^{-1} may not be that of the dusty CSE, see the discussion in Sect. 4.2). The inner shell mass loss rate agrees with the OH mass loss rate. Due to its huge radius of 1.4 ∼ 4 pc, the outer shell could be explained by sweep-up of interstellar material, as suggested by

the recent hydrodynamic simulation of Wareing et al. (2007). To summarise, we suggest that IRAS 16342-3814, while located in a very extended and cold detached outer dust shell, has an inner CSE whose mass loss rate (estimated from IR and OH emission) is roughly an order of magnitude higher than its ^{12}CO mass loss rate. The weakness of the ^{12}CO 2−1 line could be interpreted by the coldness of the CO gas, as suggested for some other very red OH/IR stars by Heske et al. (1990).

4.2. The high ^{12}CO expansion velocity

The ^{12}CO expansion velocity $V_{\rm exp}(^{12}{\rm CO}) = 46\,{\rm km\,s^{-1}}$ is too high for a typical OH/IR star (typically $\sim 15 \pm 5\,{\rm km\,s^{-1}}$ for long period OH/IR stars, see e.g., Chen et al. 2001). Another possible source of the broad ^{12}CO emission is the swept-up bipolar bubble walls. According to a momentum driven wind-interaction model suggested by Zijlstra et al. (2001), the radial motion velocity of different parts of the bubble wall will be proportional to the distance to the central star. This has been confirmed by the linear OH maser velocity offset-radius ($V-r$) relationship found by Sahai et al. (1999) and Zijlstra et al. (2001). Assuming that $V_{\rm exp}(^{12}{\rm CO})$ follows the same $V-r$ relationship in Fig. 3 of Sahai et al. (1999), we find a rough angular radius of 0.5″ for the CO emission region, similar to that of OH mainline masers. Further assuming a Gaussian source shape, the brightness temperature of the ^{12}CO 2−1 line can be estimated to be ∼30 K. Therefore, the ^{12}CO 2−1 line could be optically thin if the gas temperature is much higher than this.

Further insight can be gained by comparing the velocities of the ^{12}CO 2−1 line, OH and H_2O masers. We find several interesting facts by comparing the CO velocities with the $V-r$ relationship of OH masers in Fig. 3 of Sahai et al. (1999): 1) the 1612 MHz maser velocity offsets are all $\gtrsim V_{\rm exp}(^{12}{\rm CO})$, while most of the OH 1665/1667 MHz (mainline) maser velocity offsets $\lesssim V_{\rm exp}(^{12}{\rm CO})$; 2) the OH 1612 MHz masers show two components – a pair of bipolar high velocity clumps that tightly follow the linear $V-r$ relation and a peculiar group of points with $V_{\rm LSR} \sim 0\,{\rm km\,s^{-1}}$ but scattered in a large radius range (−1.1″∼0″); 3) the position of the bipolar 1612 MHz maser component is not symmetrical with respect to the star position, perhaps due to 3D projection effects. The peculiar group of 1612 MHz masers are not only scattered in radius, but also scattered in position angle with respect to the central star in the VLA maps (see Figs. 1b and 9 of Sahai et al. 1999; Zijlstra et al. 2001, respectively). This is difficult to explain with a spherical expanding shell model in which masers should show an elliptical relation between line-of-sight velocity and projected radial distance. Taking away this peculiar 1612 MHz maser component, one can see a better $V-r$ relationship between the remaining 1612, 1665 and 1667 MHz masers. If we further take a velocity span of $\sim 248\,{\rm km\,s^{-1}}$ and a spatial separation of ∼3″ of H_2O masers from Morris et al. (2003) and overlap their symmetry center with that of OH masers, we can see that the H_2O masers follow the same linear $V-r$ relationship quite well. Based on these arguments, we can sketch a picture for the CSE as follows:

Both the OH mainline masers and the CO emission arise from the same region near the base of the bipolar outflow, the two clumps of high velocity OH 1612 maser spots are located on the farther and faster part of the bipolar lobe side walls, the H_2O masers are stimulated by the shock fronts at the two farthest and fastest ends of the bipolar lobes, while the peculiar group of spatially scattered 1612 MHz maser spots are located in an independent structure that is blue-shifted by $\sim -46\,{\rm km\,s^{-1}}$ with respect to the star but not necessarily associated with the bipolar outflow. The dark waist and the slow AGB wind might be simply too cold to be detected in our CO 2−1 line spectra. Actually, the pair of faint spikes on the top of the broad ^{12}CO 2−1 line profile near the line centre in Fig. 1 could be the emission from the slow AGB wind. If this is true, we may estimate a crude AGB wind speed of $\sim 13\,{\rm km\,s^{-1}}$, typical for an AGB star.

4.3. On the origin of the extremely low ^{12}CO/^{13}CO ratio

The detection of the ^{13}CO $J = 2-1$ line yields an extremely small ^{12}CO/^{13}CO peak flux ratio of 1.7. A range of ^{12}CO/^{13}CO ratios have been found in PPNe and PNe by other researchers. Hasegawa (2005) concluded from a survey of published ^{13}CO observations of PNe (Palla et al. 2000; Balser et al. 2002; Bachiller et al. 1997; Josselin & Bachiller 2003) that the ^{12}CO/^{13}CO ratios are about 10∼30 in most PNe, but are 2∼3 in a few and >60 in a few others. Some examples of low ratios are: ^{12}CO/^{13}CO ∼ 4.6 in AFGL 618, ∼2.2 in M 1–16 (Balser et al. 2002), ∼3 in the PN NGC 6302 (Hasegawa & Kwok 2003), and ∼3.2 in HD 17982 (Josselin & Lèbre 2001). Bachiller et al. (1997) pointed out that the ^{12}CO/^{13}CO ratios in PPNe and PNe are affected by two competing effects: selective photodissociation of ^{13}CO and isotopic fractionation of ^{13}C in CO. Another issue is the opacity in the ^{12}CO lines, e.g., the very low ratio in NGC 6302 was later found by interferometry work of Peretto et al. (2007) to be affected by opacity effects in a massive torus and the true ^{12}C/^{13}C should be >15. For an embedded dusty post-AGB star like IRAS 16342-3814, we do not need to worry about the selective photodissociation in the central region. If the detected CO emission does come from the accelerated bipolar bubble walls (see the discussion in Sect. 4.2), neither isotopic fractionation nor ^{12}CO line opacity should be an issue, since the dynamical age of the bipolar jets is short (∼100 yr) and the high expansion velocity and high radial velocity gradient (according to the wind interaction model) might render the ^{12}CO emission not too optically thick. A rough but conservative calculation of the optical depth under an LVG approximation gives a value smaller than unity. However, better CO line data is required to confirm this. We also find that our ^{12}CO/^{13}CO ratio is about 1.1 and 3.2 in the red and blue line wings ($46 > |V_{\rm exp}| > 15\,{\rm km\,s^{-1}}$) respectively, but the uncertainties are larger there. One more issue is that the ^{12}CO and ^{13}CO lines might come from different clumps of gas. Again, better CO line profiles and, better still, CO mapping data are needed to clarify this point and thus to constrain a reliable ^{12}C/^{13}C ratio. Therefore, later in this section, we will discuss different opacity cases separately, using only the assumption that the ^{12}CO and ^{13}CO lines are co-located in the CSE.

A precise measurement of the ^{12}C/^{13}C ratio has the potential to cast light on the evolutionary status of the star. Stellar models of low mass ($M \lesssim 2.0\ M_\odot$) and intermediate mass ($2.0\ M_\odot \lesssim M \lesssim 8.0\ M_\odot$) stars (e.g., El Eid 1994; Straniero et al. 1997; Karakas & Lattanzio 2007) show that there are quite a few phases of evolution where this ratio is altered from the initial value (assumed to be solar at 89). The first occurs during the first dredge up (FDU) at the beginning of the Red Giant Branch (RGB). Here the ratio declines from the initial value to ∼20 as the convective envelope moves in and mixes up partially burnt material (we note that the second dredge-up has only a minor effect on the ratio). The second evolutionary phase that alters the ^{12}C/^{13}C ratio is not predicted by stellar models. Observations have shown that the isotopic ratio reduces along the RGB in low-mass stars ($M \lesssim 2.0\ M_\odot$), via a process known as Deep

Mixing (also known as δ_μ mixing – see the recent theoretical models by Eggleton et al. 2008). This phenomenon reduces the ratio to a value of ~15 by the end of the RGB in Population I stars. The third phase that significantly alters the ratio actually increases it – the Third Dredge-Up (TDU). Here ^{12}C is periodically mixed into the envelope during the thermally-pulsing AGB stage (TPAGB), raising the ^{12}C/^{13}C ratio from the FDU value to values of ~60 or more (see e.g., Lebzelter et al. 2008, for recent observations of this effect). The final phase to alter the ratio is Hot Bottom Burning (HBB). However this only occurs in stars more massive than ~4 or 5 $M_\odot$ (at solar metallicity). HBB is active during the later phases of the TPAGB and acts to burn the carbon and nitrogen in the convective envelope via the CNO cycles. This results in the ^{12}C/^{13}C ratio approaching the equilibrium value of ~3 (see e.g., Plez et al. 1993; McSaveney et al. 2007, for some observational evidence of this phenomenon). The very low ^{12}C/^{13}C ratio in some Galactic PNe, PPNs and extremely young post-AGB stars like IRAS 16342-3814 could be also indicative of the HBB process.

If IRAS 16342-3814 has a high ^{12}C/^{13}C ratio close to the solar value of 89 (i.e., ~50 times larger than the ^{12}CO/^{13}CO line ratio, e.g., as a 3 $M_\odot$ star experiencing TDU), the CO line optical depths can be derived from the observed ^{12}CO/^{13}CO ratio (=1.7) to be $\tau(^{12}\mathrm{CO}) \sim 82$ and $\tau(^{13}\mathrm{CO}) \sim 0.93$ (according to $T \propto (1 - \mathrm{e}^{-\tau})$ under the assumption of co-location of ^{12}CO and ^{13}CO gas and the same excitation temperature). However, the ^{12}CO mass loss rate should also be raised by a factor of $\tau/(1 - \mathrm{e}^{-\tau}) = 82$ to 5.7~45.9×10^{-5} $M_\odot$/yr, which is significantly higher than the OH and IR mass loss rates.

If the true ^{12}C/^{13}C ratio is an intermediate value of 20, i.e., a factor of ~10 higher than the ^{12}CO/^{13}CO line ratio, the similarly determined opacities are $\tau(^{12}\mathrm{CO}) \sim 19$ and $\tau(^{13}\mathrm{CO}) \sim 0.93$. In this case, the ^{12}CO mass loss rate is comparable to the OH and IR mass loss rates. Therefore, a low mass AGB star ($\lesssim$1.5 $M_\odot$) that did not experience TDU or HBB and thus retains its FDU plus deep mixing surface abundances would be a possible progenitor of IRAS 16342-3814.

If the ^{12}CO 2–1 line is only slightly optically thick so that the ^{12}C/^{13}C ratio is ~3 (the CNO equilibrium value), the CO line opacities are $\tau(^{12}\mathrm{CO}) \sim 2.3$ and $\tau(^{13}\mathrm{CO}) \sim 0.77$. In this case, we can see that the only process (to the best of our knowledge) that could have lowered the ^{12}C/^{13}C ratio to such a value is HBB. Thus the inferred mass of the star that produced the material that we observe today would have been >4 or 5 $M_\odot$. Interestingly, the low ^{12}CO/^{13}CO ratio, bipolar outflow, and the properties of the OH masers of IRAS 16342-3814 are reminiscent of the massive PPN IRAS 22036+5306 investigated by Sahai et al. (2003, 2006), although IRAS 16342-3814 is probably in an earlier phase of evolution due to the presence of the young "water fountain". Alternatively, a binary system in which a massive AGB star had transfered low ^{12}C/^{13}C matter to the current AGB star is also possible. We note that a low isotopic ratio is supported by our rough estimation of the low ^{12}CO 2–1 opacity at the beginning of this section.

However, both the measured CO and H_2O maser systemic velocities (~44 km s^{-1}, Likkel et al. 1992) confirm that the spatial motion of IRAS 16342-3814 is in the reverse direction of the Galactic disk rotation (interstellar CO cloud velocity near the same line of sight is ~−17 km s^{-1}, Dame et al. 2001). The peculiar stellar motion lends weight to IRAS 16342-3814 being a low mass star, although in rare cases kick-out of stars from the crowded galactic plane can give rise to peculiar velocities.

Given the preceeding discussions it is obvious that further observations are highly desirable to investigate the different opacity possibilities. Molecular line interferometry and maser proper motion measurements (such as the work of Imai et al. 2007) are also needed to check the interstellar contamination, confirm the co-location of the ^{12}CO and ^{13}CO gas, and to locate the birthplace of the possibly escaped AGB progenitor on the Galactic plane.

Acknowledgements. We thank ARO telescope operators for the assistance in remote observations. J.H. acknowledge the projects Nos. 10433030 and 10503011 of the National Natural Science Foundation of China. T.I. acknowledges the support from NSC grant NSC 96-2112-M-001-018-MY3. The SMT is operated by the Arizona Radio Observatory (ARO), Steward Observatory, University of Arizona.

References

Bachiller, R., Forveille, T., Huggins, P. J., & Cox, P. 1997, A&A, 324, 1123
Balser, D. S., McMullin, J. P., & Wilson, T. L. 2002, ApJ, 572, 326
Baud, B., & Habing, H. J. 1983, A&A, 127, 73
Chen, P. S., Szczerba, R., Kwok, S., & Volk, K. 2001, A&A, 368, 1006
Claussen, M., Sahai, R., & Morris, M. 2004, in Asymmetrical Planetary Nebulae III: Winds, Structure and the Thunderbird, ed. M. Meixner, J. H. Kastner, B. Balick, & N. Soker, ASP Conf. Ser., 313, 331
Dame, T. M., Hartmann, D., & Thaddeus, P. 2001, ApJ, 547, 792
Dijkstra, C., Waters, L. B. F. M., Kemper, F., et al. 2003, A&A, 399, 1037
Do, T., Morris, M., Sahai, R., & Stapelfeldt, K. 2007, AJ, 134, 1419
Eggleton, P. P., Dearborn, D. S. P., & Lattanzio, J. C. 2008, ApJ, 677, 581
El Eid, M. F. 1994, A&A, 285, 915
Hasegawa, T. 2005, in Planetary Nebulae as Astronomical Tools, ed. R. Szczerba, G. Stasińska, & S. K. Gorny, AIP Conf. Ser., 804, 218
Hasegawa, T. I., & Kwok, S. 2003, ApJ, 585, 475
Heske, A., Forveille, T., Omont, A., van der Veen, W. E. C. J., & Habing, H. J. 1990, A&A, 239, 173
Imai, H. 2007, in IAU Symp., 242, 279
Imai, H., Sahai, R., & Morris, M. 2007, ApJ, 669, 424
Josselin, E., & Bachiller, R. 2003, A&A, 397, 659
Josselin, E., & Lèbre, A. 2001, A&A, 367, 826
Karakas, A., & Lattanzio, J. C. 2007, PASA, 24, 103
Knapp, G. R., & Morris, M. 1985, ApJ, 292, 640
Lebzelter, T., Lederer, M. T., Cristallo, S., et al. 2008, ArXiv e-prints, 805
Likkel, L., & Morris, M. 1988, ApJ, 329, 914
Likkel, L., Morris, M., & Maddalena, R. J. 1992, A&A, 256, 581
McSaveney, J. A., Wood, P. R., Scholz, M., Lattanzio, J. C., & Hinkle, K. H. 2007, MNRAS, 378, 1089
Morris, M. R., Sahai, R., & Claussen, M. 2003, in Rev. Mex. Astron. Astrofis. Conf. Ser., ed. J. Arthur, & W. J. Henney, 15, 20
Palla, F., Bachiller, R., Stanghellini, L., Tosi, M., & Galli, D. 2000, A&A, 355, 69
Peretto, N., Fuller, G., Zijlstra, A., & Patel, N. 2007, A&A, 473, 207
Plez, B., Smith, V. V., & Lambert, D. L. 1993, ApJ, 418, 812
Sahai, R., Te Lintel Hekkert, P., Morris, M., Zijlstra, A., & Likkel, L. 1999, ApJ, 514, L115
Sahai, R., Zijlstra, A., Sánchez Contreras, C., & Morris, M. 2003, ApJ, 586, L81
Sahai, R., Le Mignant, D., Sánchez Contreras, C., Campbell, R. D., & Chaffee, F. H. 2005, ApJ, 622, L53
Sahai, R., Young, K., Patel, N. A., Sánchez Contreras, C., & Morris, M. 2006, ApJ, 653, 1241
Straniero, O., Chieffi, A., Limongi, M., et al. 1997, ApJ, 478, 332
Szymczak, M., & Gérard, E. 2004, A&A, 423, 209
Te Lintel Hekkert, P., Habing, H. J., Caswell, J. L., Norris, R. P., & Haynes, R. F. 1988, A&A, 202, L19
Wareing, C. J., Zijlstra, A. A., & O'Brien, T. J. 2007, MNRAS, 382, 1233
Zijlstra, A. A., Chapman, J. M., Te Lintel Hekkert, P., et al. 2001, MNRAS, 322, 280